A Volcano Rekindled: The Renewed Eruption of Mount St. Helens, 2004–2006
Edited by David R. Sherrod, William E. Scott, and Peter H. Stauffer
U.S. Geological Survey Professional Paper 1750, 2008

Chapter 34

Plagioclase Populations and Zoning in Dacite of the 2004–2005 Mount St. Helens Eruption: Constraints for Magma Origin and Dynamics

By Martin J. Streck[1], Cindy A. Broderick[1], Carl R. Thornber[2], Michael A. Clynne[3], and John S. Pallister[2]

Abstract

We investigated plagioclase phenocrysts in dacite of the 2004–5 eruption of Mount St. Helens to gain insights into the magmatic processes of the current eruption, which is characterized by prolonged, nearly solid-state extrusion, low gas emission, and shallow seismicity. In addition, we investigated plagioclase of 1980–86 dacite.

Light and Nomarski microscopy were used to texturally characterize plagioclase crystals. Electron microprobe analyses measured their compositions. We systematically mapped and categorized all plagioclase phenocrysts in a preselected area according to the following criteria: (1) occurrence of zones of acicular orthopyroxene inclusions, (2) presence of dissolution surface(s), and (3) spatial association of 1 and 2. Phenocrysts fall into three main categories; one category contains four subcategories.

The range of anorthite (An) content in 2004–5 plagioclase is about $An_{57–35}$ during the last 30–40 percent crystallization of plagioclase phenocrysts. Select microphenocrysts (10–50 μm) range from An_{30} to An_{42}. Anorthite content is lowest near outermost rims of phenocrysts, but zonation patterns between interior and rim indicate variable trends that correlate with textural features. Crystals without dissolution surfaces (about 14 percent of total) show steadily decreasing An content outward to the crystal rim (outer ~80 μm). All other crystals are banded as a consequence of dissolution; dissolution surfaces are band boundaries. Such crystals display normal outward An zoning within a single band that, following dissolution, is then overgrown abruptly by high-An material of the next band. Swarms of acicular orthopyroxene inclusions in plagioclase are characteristic of 2004–5 dacite. They occur mostly inward of dissolution surfaces, where band composition reaches lowest An content. The relative proportions of the three crystal types are distinctly different between 2004–5 dacite and 1980s dome dacite.

We propose that crystals with no dissolution surfaces are those that were supplied last to the shallow reservoir, whereas plagioclase with increasingly more complex zoning patterns (that is, the number of zoned bands bounded by dissolution surfaces) result from prolonged residency and evolution in the reservoir. We propose that banding and An zoning across multiple bands are primarily a response to thermally induced fluctuations in crystallinity of the magma in combination with recharge; a lesser role is ascribed to cycling crystals through pressure gradients. Crystals without dissolution surfaces, in contrast, could have grown only in response to steady(?) decompression. Some heating-cooling cycles probably postdate the final eruption in 1986. They resulted from small recharge events that supplied new crystals that then experienced resorption-growth cycles. We suggest that magmatic events shortly prior to the current eruption, recorded in the outermost zones of plagioclase phenocrysts, began with the incorporation of acicular orthopyroxene, followed by last resorption, and concluded with crystallization of euhedral rims. Finally, we propose that 2004–5 dacite is composed mostly of dacite magma that remained after 1986 and underwent subsequent magmatic evolution but, more importantly, contains a component of new dacite from deeper in the magmatic system, which may have triggered the new eruption.

Introduction

The 2004 eruption of Mount St. Helens is remarkable for several reasons. Nearly solid, gas-poor dacite lava has been

[1] Department of Geology, Portland State University, Portland, OR 97207

[2] U.S. Geological Survey, 1300 SE Cardinal Court, Vancouver, WA 98683

[3] U.S. Geological Survey, 345 Middlefield Road, Menlo Park, CA 94025

extruded continuously for 28 months (at time of this writing, early 2007). Earthquakes are limited to the upper 3 km, with most located less than 1 km below the surface; no deeper seismicity has been observed (Moran and others, this volume, chap. 2). Emissions of SO_2, H_2S, and CO_2 are extremely low, indicating eruption of degassed magma (Gerlach and others, this volume, chap. 26). Low gas emission argues against the possibility of proximal mafic magma at depth, which might be called upon to have initiated the current eruption, and is consistent with an apparent lack of direct evidence for mingling with more mafic magma. This combination raises two important questions: (1) what is the driving force for the current eruption, and (2) is there petrologic evidence for magma recharge as an eruption trigger?

We studied plagioclase phenocrysts in 2004–5 dacite (fig. 1) and 1980–86 dacite dome rocks with the goal of using these data to investigate magma origin and reservoir dynamics, including evidence for recharge. We used polarized light and Nomarski microscopy in combination with detailed microprobe traverses to texturally and compositionally characterize single plagioclase crystals, focusing on areas near phenocryst rims. In addition, we systematically mapped and classified all plagioclase phenocrysts along thin-section traverses to evaluate variability in plagioclase crystal populations. On the basis of these datasets, we infer that the new dacite is composed of three components. The first is magma that remained in the reservoir after 1986 and whose plagioclase crystals typically underwent crystallization and resorption as crystals cycled through cooler and hotter (and possibly deeper) parts of the reservoir, respectively. Whether or not some of this magma was isolated and escaped any modification remains open to debate. The second component is magma that was probably supplied recently by recharge of the shallow Mount St. Helens magma chamber. This magma carried plagioclase phenocrysts that grew continuously and are compatible with crystallization controlled largely by decompression (Blundy and Cashman, 2001). In addition to these magmatic components, there is evidence that some plagioclase in erupting dacite magmas was derived by disintegration of wall-rock xenoliths constituting the third component. These include crystals with distinct sieve-textured cores probably derived from gabbroic source rocks (Heliker, 1995) and older Mount St. Helens dacite containing plagioclase with unusually low An content and sporadically hosting quartz inclusions (M.J. Streck, unpub. data; Clynne and others, this volume, chap. 28). Our data are compatible with recharge-driven initiation of the current eruption. We suggest that new magma is dacite and is hotter than and has fewer crystals than the resident dacite with which it has blended.

Samples and Analytical Procedures

Samples for this study are splits of samples collected by the staff of the Cascades Volcano Observatory (CVO) as the eruption proceeded (table 1). We report collection dates for 2004–5 samples and eruption dates for 1980–86 samples. The full sample names are given in table 1 but are abbreviated. The reader is referred to Pallister and others (this volume, chap. 30) for information about likely eruption dates for 2004–5 samples. For most of our samples, the estimated eruption date precedes collection date by 1–3 weeks. Sample localities are

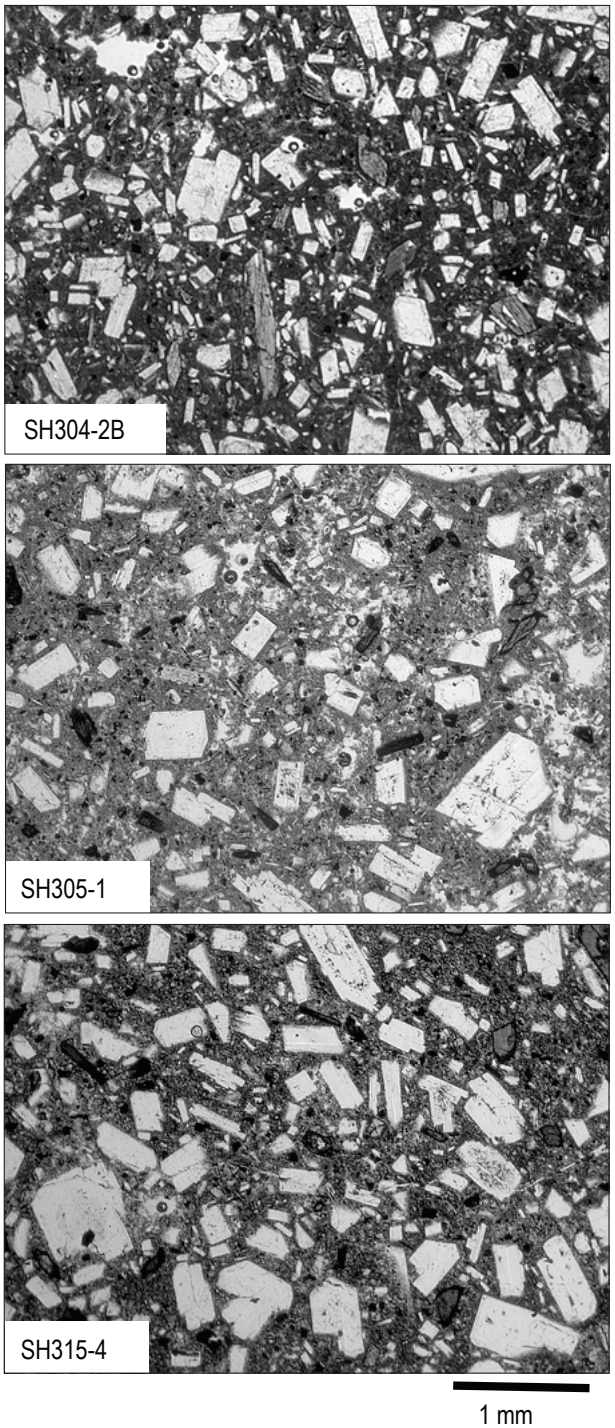

Figure 1. Thin sections of dacite from 2004–5 Mount St. Helens eruption showing crystal-rich nature and plagioclase occurrence mostly as single, equant phenocrysts. Note sporadic plagioclase with sieved interior and clear overgrowth.

Table 1. Samples analyzed in this study and results of crystal mapping.

[All plagioclase assigned to crystal type: Type 1, dissolution surfaces; Type 2, dissolution surfaces and acicular orthopyroxene (opx); Type 3, no dissolution surface and with or without acicular opx. Type 2 crystals further grouped by position of acicular opx relative to dissolution surface(s): A, opx abundant at outermost dissolution surface; B, opx at some surface inboard of the outermost; C, opx is near rim but dissolution surface is near core of crystal; D, opx is near core but dissolution surface is near rim of crystal. EMP, electron microprobe analyses; dashes indicate no analysis. Column for sheets shows total number of images from two transects across each thin section (see fig. 2). Column for indeterminate crystals shows proportion (percent) of unresolved assignments relative to total plagioclase content.]

2004–5 Dacite samples							Normalized abundance, in %, with parenthetical 1σ deviation				Dissolution association in Type 2 crystals, in % (see table notes)			
Sample No.	Collection date	EMP analyses	Sheets per thin section	Total crystals examined	Crystals per sheet	1σ dev.	Type 1 crystals	Type 2 crystals	Type 3 crystals	Indeterminate crystals	A	B	C	D
SH304-2B	Nov. 4, 2004	16	17	1,939	114	17	66 (7)	24 (7)	10 (5)	12	70	18	11	2
SH305-1	Jan. 3, 2005	6	16	1,118	70	8	40 (6)	29 (6)	31 (6)	20	75	9	12	4
SH308-3	Feb. 22, 2005	--	18	1,653	92	12	52 (6)	28 (8)	20 (6)	11	70	11	18	2
SH311-1B	Jan. 19, 2005	9	--	--	--	--	--	--	--	--	--	--	--	--
SH315-4	Apr. 19, 2005	8	13	1,354	104	21	57 (11)	34 (10)	9 (4)	8	69	21	11	0
SH321	Aug. 19, 2005	--	17	1,275	75	18	52 (5)	37 (7)	11 (5)	5	69	23	6	2
SH323-2	Oct. 18, 2005	--	16	1,213	76	15	65 (6)	27 (6)	8 (2)	7	82	14	4	0
SH324-3	Dec. 15, 2005	--	16	1,290	81	6	66 (5)	28 (4)	6 (3)	5	77	20	3	0
						average	57 (10)	30 (4)	14 (9)					

1980–86 Dacite samples							Normalized abundance, in %, with parenthetical 1σ deviation				Dissolution association in Type 2 crystals, in % (see table notes)			
Sample No.	Eruption date	EMP analyses	Sheets per thin section	Total crystals examined	Crystals per sheet	1σ dev.	Type 1 crystals	Type 2 crystals	Type 3 crystals	Indeterminate crystals	A	B	C	D
SH226	October 1986	--	17	747	44	12	80 (10)	4 (3)	16 (9)	16	36	36	28	0
SH157	June 1984	--	15	490	33	7	91 (4)	5 (3)	4 (3)	7	14	81	0	5
SH131	August 1982	--	10	326	33	6	88 (7)	5 (5)	7 (4)	12	19	75	6	0
SC334-99B	~April 1981	9	14	835	60	8	89 (4)	1 (1)	10 (4)	16	50	50	0	0
SH52	December 1980	--	10	181	18	6	84 (9)	9 (6)	7 (5)	11	8	67	0	25
						average	86 (6)	5 (3)	9 (6)					

shown on photogeologic maps in Herriott and others (this volume, chap. 10).

We prepared polished thin sections that were etched in concentrated hydrofluoroboric acid for 25 s in preparation for Nomarski differential interference contrast (NDIC or Nomarski, for brevity) microscopy. This microscopy, in combination with transmitted-light microscopy, was employed to investigate textural aspects of plagioclase crystals. To associate textural characteristics with composition, we performed microprobe analyses along traverses in crystals representative of the range of textural features displayed. Point spacing along analytical traverses was 3–4 μm, concentrating on the outer ~100 μm of the crystal. We analyzed 39 crystals from 2004–5 samples and 9 crystals from 1981 dome lava (table 1). Analyses were done using the five-spectrometer CAMECA SX100 electron microprobe housed at Oregon State University, which was mostly operated remotely from Portland State University. Some additional crystals were analyzed in single-point mode at the University of Stuttgart, Germany, to characterize very small plagioclase crystals. Natural mineral standards were used to calibrate the instruments. Analytical conditions included an accelerating voltage of 15 kV, a beam current of 15 nA, and a focused (~1 μm diameter) beam. Collection times on peak and background positions were 10 and 5 s for Na (counted first), Si, Al, and Ca; times were 30 and 15 s for K, Mg, and Fe.

Encouraged by initial efforts to categorize plagioclase phenocrysts into different textural types (see below), we designed a mapping procedure to determine proportions of plagioclase crystal types. For each thin section, we used transmitted-light images at magnification × 25 and mapped two separate transects, comprising a total of 10–18 adjacent images, or sheets (table 1, fig. 2). In each × 25 sheet, we inspected every plagioclase phenocryst (≥80 μm) with transmitted and Nomarski microscopy and categorized crystals according to selected textural features. In this way, we obtained textural data on all plagioclase phenocrysts within an area covering roughly one-third of each thin section (table 1).

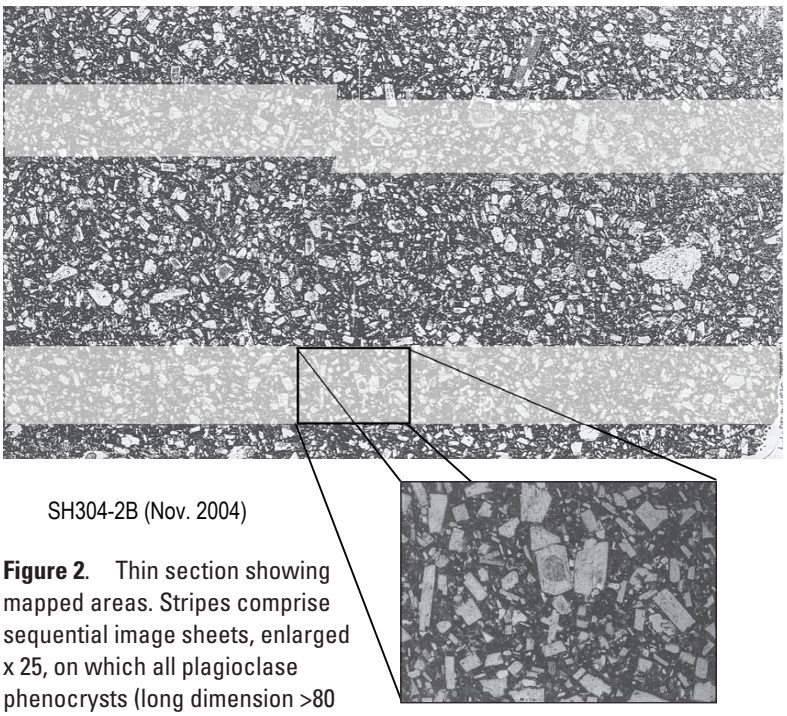

Figure 2. Thin section showing mapped areas. Stripes comprise sequential image sheets, enlarged x 25, on which all plagioclase phenocrysts (long dimension >80 μm) were classified.

Plagioclase in 2004–2005 Mount St. Helens Dacite

The phenocryst assemblage of 2004–5 dacite is dominated by plagioclase with subordinate amounts of orthopyroxene, amphibole, and Fe–Ti oxides. Plagioclase consists dominantly (≥90 percent) of single, euhedral, clear, equant phenocrysts 80–800 μm across (fig. 1). Equant plagioclase also occurs as smaller crystals between 80 and 10 μm. We call these microphenocrysts even though they overlap in size with microlites in the surrounding interstitial groundmass. A few plagioclase crystals are texturally (and likely compositionally) distinct. Typically these are considerably larger (≥1 mm), subhedral to anhedral, and commonly display a sieved-textured interior. Plagioclase glomerocrysts are rare.

Textural Features

Individual plagioclase phenocrysts are characterized by growth features in the form of oscillatory zoning (parallel lines in Nomarski images) or by practically textureless parts (thus appearing as flat areas in Nomarski images) (fig. 3). Resorption textures are commonly found within crystals as dissolution surfaces that cut obliquely across oscillatory growth zones (figs. 3*A*–*D*) (note: we use the term "resorption" for the general process that creates a "dissolution surface"). The extent of resorption varies and most commonly is expressed as variable degrees of rounding of the corners of interior zones within a crystal. Commonly the phenocrysts have multiple dissolution surfaces; examples with four or more were observed. Sieved or pitted textures are rare in crystals of the dominant population, especially near their rims, but occur frequently in the interiors of the large crystals (>800 μm). Plagioclase phenocrysts may contain inclusions of orthopyroxene, Fe–Ti oxide, amphibole, apatite, and glass (melt). A characteristic feature of plagioclase of the 2004–5 eruption is the occurrence and distribution of tiny orthopyroxene inclusions. They are acicular, with length-to-width ratios of ~10 or greater. Their length is variable but typically about 30 μm. Their maximum widths are on the order of 4–5 μm. Acicular orthopyroxene inclusions occur mostly

in swarms and are concentrated in bands close to dissolution surfaces (figs. 3*C*, 3*D*), although they also occur independently of the surfaces (figs. 3*E*, 3*F*). Where associated with a dissolution surface, acicular orthopyroxene bands are, in most cases, inward of the dissolution surface, toward the center of the crystal (figs. 3, 4).

Compositional Features

The overall compositional range for the outer 80–100 μm of plagioclase phenocrysts in the 2004–5 dacite ranges from $An_{32–38}$ to $An_{55–60}$ (figs. 4, 5, 6). At or near the rim (that is, within one traverse step of ~3 μm), compositions are

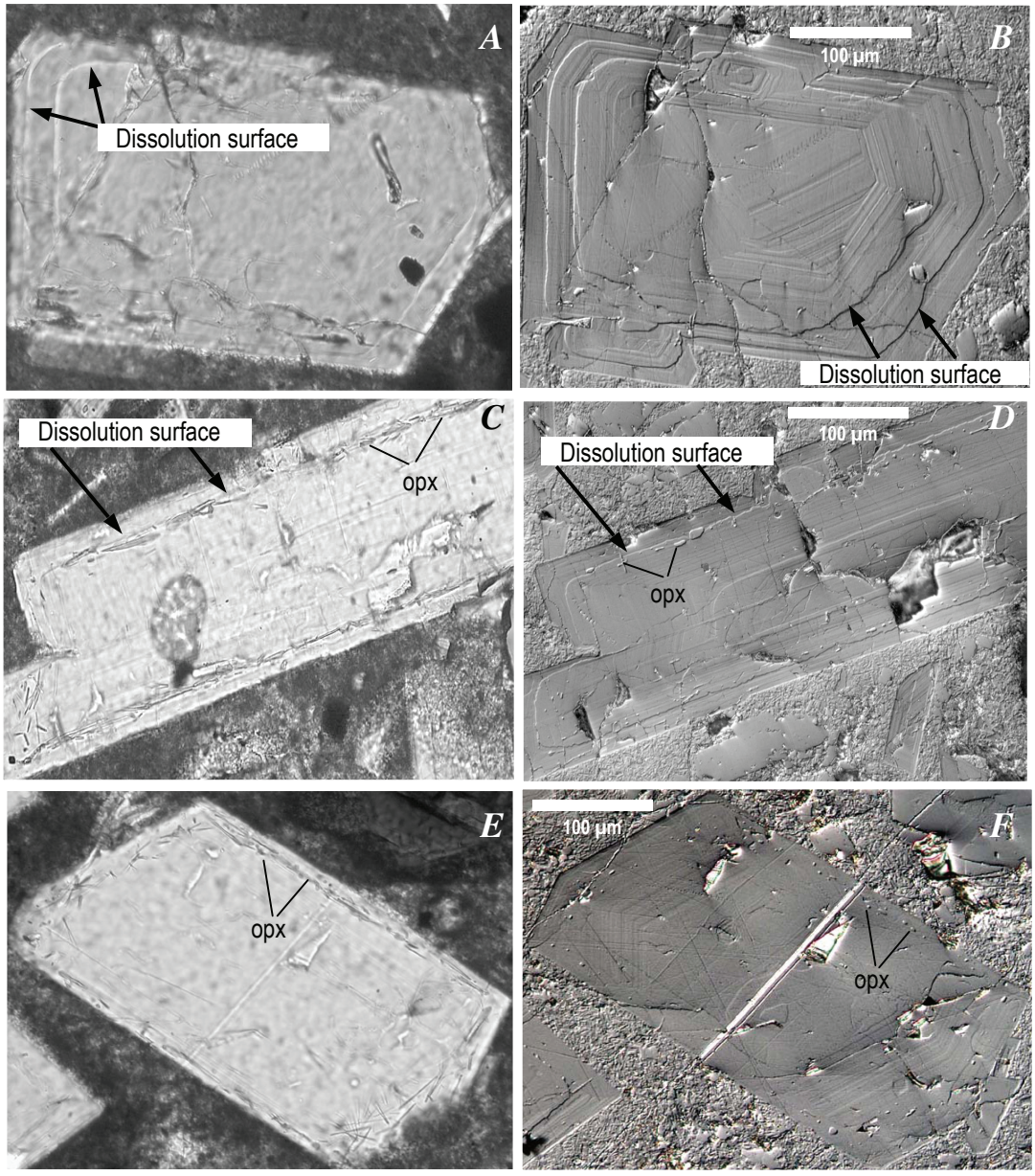

Figure 3. Plagioclase types distinguished by combination of dissolution surfaces (arrows) and presence of acicular orthopyroxene inclusions (opx). Scale bars are 100 μm. Left column, transmitted light images; right column, corresponding Nomarski differential interference contrast images. *A*, *B*, Type 1 plagioclase, with two dissolution surfaces but without acicular orthopyroxene inclusions. *C*, *D*, Type 2 plagioclase, with acicular orthopyroxene inclusions inbound of dissolution surface. *E*, *F*, Type 3 plagioclase with no dissolution surface but containing, in this example, acicular orthopyroxene inclusions near rim.

$An_{35–44}$, although $An_{37–38}$ is most common. Analyzed microphenocrysts are 10 to 50 μm in size and range from ~An_{30} to ~An_{42} (fig. 6). Compositions of microphenocrysts or at the rims of phenocrysts in 2004–5 samples have a wider range in An content than that reported for samples of 1980s dome dacite (Cashman, 1992), but one of our comparison samples of 1980–86 dome dacites (SC-99-334b; table 1, fig. 6) suggests a similar range with minima of $An_{38–40}$ and maxima of $An_{60–65}$ and outermost rim compositions of $An_{35–48}$. We exclude the large and sieve-textured plagioclase crystals from our analysis because they are thought to be derived from disaggregated plutonic or cumulate inclusions (Heliker, 1995). Contrasting with the above range in An content of phenocrysts are fairly sodic compositions of $An_{24–32}$ that we found in the interior parts of some phenocrysts. Such phenocrysts have not been reported previously from Mount St. Helens dacite. They are compositionally distinct but texturally indistinguishable from typical phenocrysts unless they contain abundant mineral inclusions (some of which are acicular). We also exclude these because we believe that the unusually sodic crystal interiors represent recycled older crystals derived from more-silicic magma (see below).

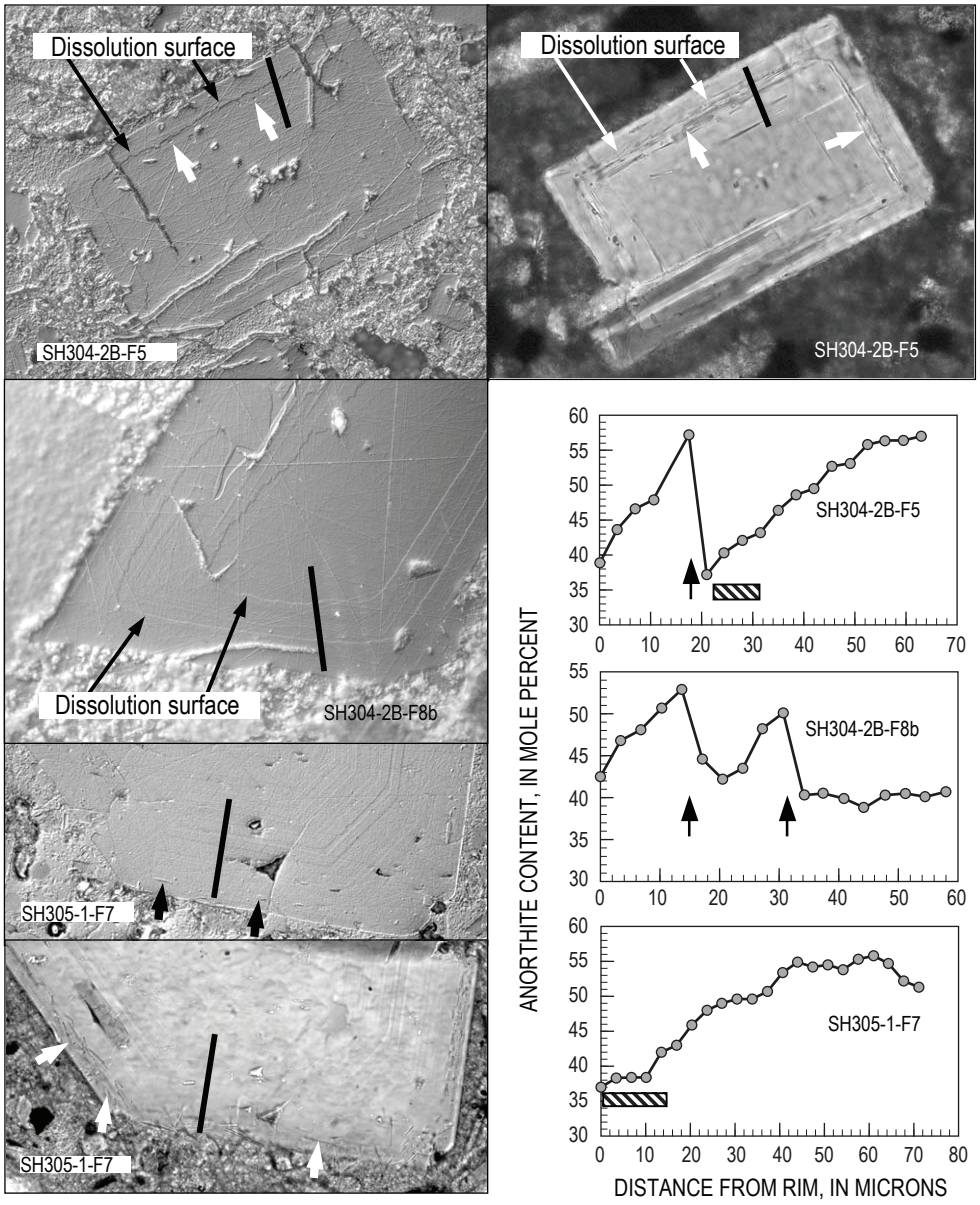

Figure 4. Correlation of textures and composition. Solid lines on Nomarski images indicate location of analytical traverses, and short arrows point to acicular orthopyroxene inclusions. Arrows in graphs indicate location of dissolution (resorption) surfaces, and bars show location of acicular orthopyroxene inclusions.

Near their rims, all plagioclase phenocrysts are compositionally normally zoned within bands that show oscillatory zoning or flat textures. We distinguish compositional from textural zoning because texturally flat areas are frequently compositionally zoned (for example, fig. 4, sample SH304-2B-F5; table 2). Band boundaries are dissolution surfaces. Band widths are variable and can be as narrow as ~10–15 μm. Some smaller crystals do not show any dissolution surface and therefore can be considered to consist of a single, broader band (about 200–300 μm). Compositional changes within a single band, regardless of width, in most cases display An decreases from 7 to 20 mol percent and thus may encompass the entire range of An variability of plagioclase in 2004–5 dacite (table 2). Compositionally uniform bands and bands with slight reverse zoning ($\Delta \sim An_5$) are rare. The initial overgrowth on a dissolution surface always has the highest An content; last growth is the lowest An content

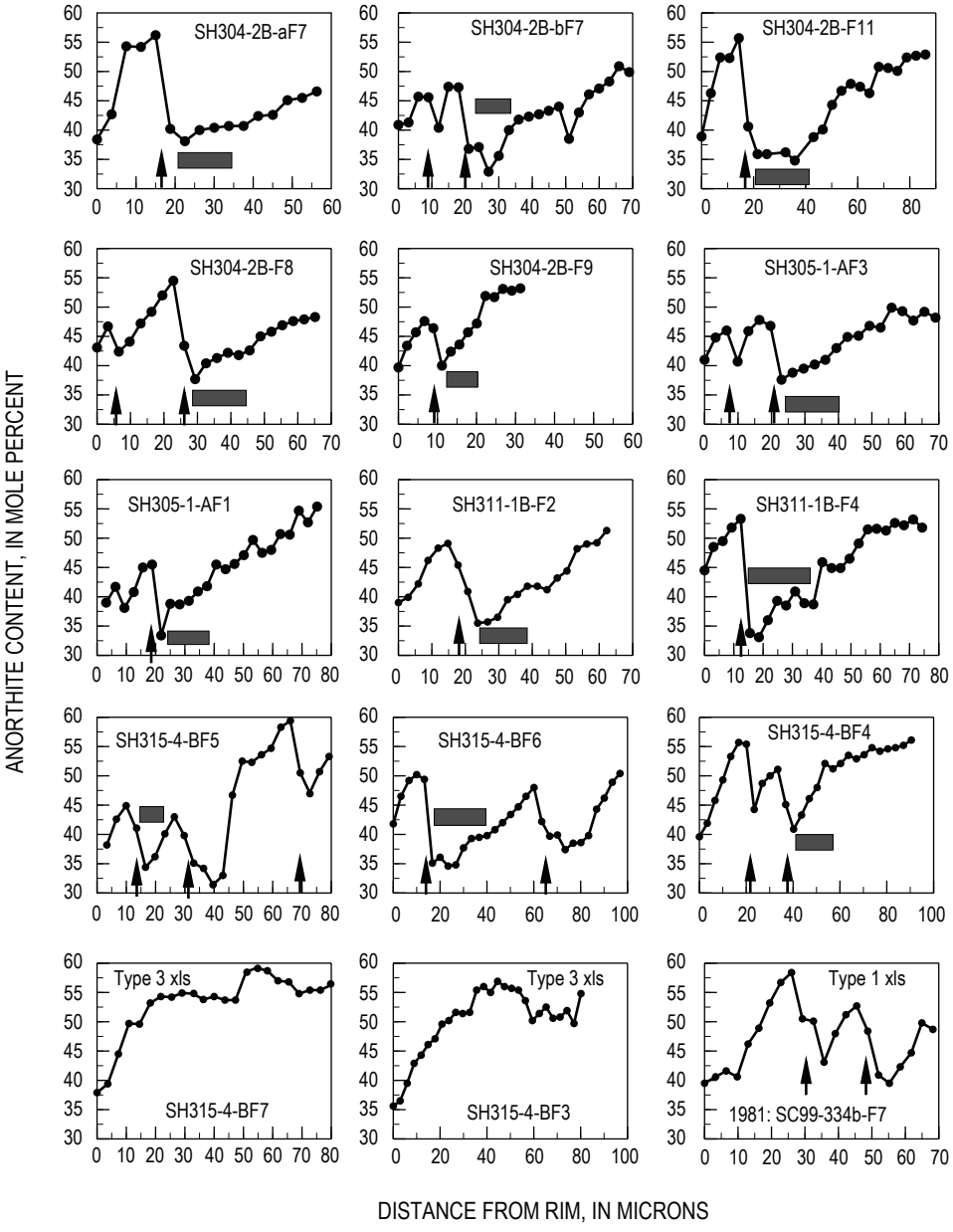

Figure 5. An profiles of Type 2 crystals—those with dissolution surfaces and acicular orthopyroxene inclusions—except bottom row, which depicts two Type 3 crystals (no resorption). Lower right, one 1981 Type 1 crystal (dissolution surface but no inclusions). Arrows indicate location of dissolution surface and bars show location of acicular orthopyroxene inclusions. Resorption is typically followed by abrupt increase in An content. Sequential growth is rimward, toward left on each graph.

within a band—a feature also observed in May 18, 1980, dacite (Pearce and others, 1987). In fact, it is an often-observed feature in volcanic plagioclase with dissolution surfaces (Pearce, 1994). Along a single analytical traverse, abrupt An increases of 5 to 25 mol percent were observed where crossing from the lowest An content of an inner band to the highest An content of the next outer band (figs. 4, 5). Thus the profiles undulate, depending on whether one or multiple dissolution surfaces exist. Rarely, overgrowth on a more interior dissolution surface can be of distinctly lower An content than inward of the dissolution surface.

Acicular orthopyroxene inclusions are consistently associated with the lower-An parts of bands. They occur where the plagioclase composition reaches $An_{33–40}$. The composition of acicular orthopyroxene inclusions is similar to the composition of orthopyroxene phenocrysts (table 3), although Al and perhaps Ca are slightly higher. It is uncertain whether the Ca and Al variation of acicular inclusions compared to orthopyroxene phenocrysts is significant given the spatial difficulties in analyzing small crystals embedded in plagioclase.

Crystal Mapping

The mapped crystal populations are distinguished by presence or absence of near-rim features produced by alternating growth and resorption events and by the presence or absence of acicular orthopyroxene inclusions. On the basis of these features, we can distinguish three crystal types and determine their proportions (table 1):

- Most abundant are plagioclase crystals containing one or several dissolution surfaces but lacking acicular orthopyroxene; they are designated Type 1 crystals.
- Second in abundance are plagioclase crystals that show dissolution surfaces and contain acicular orthopyroxene inclusions; they are designated Type 2 crystals. We further distinguished subcategories of Type 2 crystals according to location of the orthopyroxene inclusions with respect to dissolution surfaces: (A) inboard of last dissolution surface, (B) only associated with an older dissolution surface, (C) near the rim and not associated with a dissolution surface (that is, the dissolution surface is near the core of the crystals and orthopyroxene inclusions occur near the rim), and (D) near the crystal core and the dissolution surface is near rim.
- Least abundant are crystals lacking clearly discernible dissolution surfaces; they are designated Type 3 crystals. For the Type 3 category, we established subcategories based on whether acicular orthopyroxene inclusions are present or absent.

In some cases, categorization was difficult owing to poor crystal polish, fracturing, disadvantageous cutting of the crys-

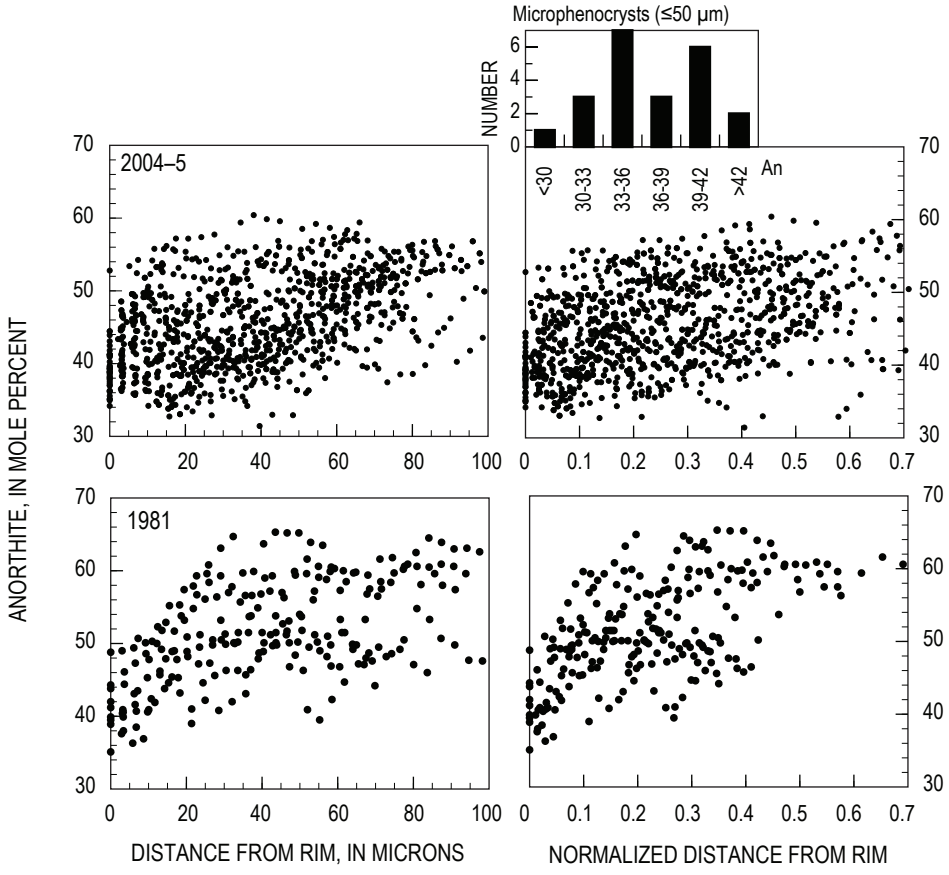

Figure 6. Anorthite content in plagioclase, showing all data of this study. Plots in left column show An content versus distance to rim; in right column, An content versus normalized distance to rim. To normalize distance to rim, we connected traverse end point at rim with center of crystals and took fraction that was covered by traverse. We projected beginning of traverse into "rim – center" line along growth zones in case where analysis traverse was not parallel to "rim – center" line. Histogram shows plagioclase composition of 22 microphenocrysts (~<50 µm) in SH321 (table 1), similar to the two observed in center and along left side of groundmass picture of sample SC99-334A shown in figure 8*A*. All microphenocrysts were analyzed in center and rim.

Table 2. Representative plagioclase compositions along profiles of two crystals shown in figure 4, starting at ~30 μm from the rim.

[FeO*, total iron as Fe^{2+}. Molecular components for plagioclase shown calculated: An, anorthite; Ab, albite; Or, orthoclase.]

SH304-2B-F5 (Type 2 crystal)										
Distance to rim (μm)-------	31.5	28.0	24.5	21.0	17.5	14.0	10.5	7.0	3.5	0
SiO_2	58.3	58.7	59.1	60.1	54.9	55.7	57.1	57.5	58.4	59.8
Al_2O_3	26.7	26.3	26.2	25.4	28.6	27.6	27.0	26.8	26.4	25.4
FeO*	0.29	0.28	0.34	0.30	0.50	0.48	0.47	0.48	0.45	0.49
MgO	0.01	0.01	0.02	0.02	0.04	0.04	0.04	0.03	0.03	0.02
CaO	8.7	8.5	8.2	7.5	11.6	10.6	9.7	9.4	8.8	7.8
Na_2O	6.2	6.4	6.6	6.9	4.8	5.2	5.7	5.9	6.2	6.7
K_2O	0.18	0.20	0.21	0.23	0.12	0.13	0.15	0.17	0.20	0.29
Total	100.3	100.3	100.6	100.4	100.5	99.9	100.2	100.2	100.5	100.5
An	43.2	42.1	40.4	37.2	57.2	52.6	47.9	46.6	43.7	38.8
Ab	55.7	56.8	58.3	61.4	42.1	46.7	51.3	52.4	55.1	59.5
Or	1.1	1.2	1.2	1.4	0.7	0.8	0.9	1.0	1.2	1.7

SH305-1-F7 (Type 3 crystal)										
Distance to rim (μm)------	30.4	27.0	23.7	20.3	16.9	13.5	10.1	6.8	3.4	0
SiO_2	55.5	55.6	55.8	56.5	56.8	57.5	58.0	58.1	58.7	58.9
Al_2O_3	27.8	28.1	27.8	27.2	26.9	26.7	26.2	25.5	25.7	25.8
FeO*	0.27	0.34	0.33	0.22	0.35	0.30	0.28	0.79	0.27	0.34
MgO	0.01	0.01	0.01	0.01	0.01	0.02	0.02	0.51	0.04	0.01
CaO	9.9	9.8	9.7	9.1	8.4	8.5	7.7	7.5	7.6	7.5
Na_2O	5.5	5.5	5.7	5.8	6.1	6.4	6.7	6.5	6.7	6.9
K_2O	0.14	0.14	0.16	0.19	0.18	0.19	0.23	0.22	0.23	0.25
Total	99.2	99.5	99.5	99.0	98.6	99.7	99.2	99.2	99.2	99.7
An	49.6	49.0	48.0	45.9	43.0	42.0	38.4	38.4	38.3	37.0
Ab	49.5	50.1	51.1	53.0	55.9	56.8	60.2	60.2	60.4	61.5
Or	0.8	0.8	0.9	1.1	1.1	1.1	1.4	1.3	1.4	1.5

tal leading to obliteration near the rim, and other ambiguities. Crystals that could not be categorized clearly are considered indeterminate crystals; their proportions ranged from 5 to 20 percent (table 1). In subsequent analysis, we assumed that the indeterminate crystals are proportionally distributed among the other populations and therefore normalized the other three categories to their sum to investigate changes in their proportions.

Comparing mapping results among sheets (images at × 25 magnification) that make up surveyed transects yielded standard deviations of mapped crystal types for a single thin section (table 1); 1σ standard deviations are typically on the order of 5–10 percent of the normalized abundance, and this appears to be the natural variation on the level of a single thin section, including the error associated with recognition.

An exception to Type 1 and Type 2 crystals being first and second in abundance is sample SH305-2 (lava collected Jan. 3, 2005), in which Type 3 crystals are slightly more abundant or subequal to Type 2 crystals (fig. 7).

Variations among crystal types in samples of the 2004–5 dacite indicate some trends after apparent natural variation within individual samples (based on 1σ errors) is taken into consideration. Notable are (1) an increase in the abundance of Type 3 crystals in SH305, which taper back to the level observed at the onset of the eruption at the expense of Type 1 crystals, and (2) a possible slight increase in the abundance of Type 2 crystals from SH304 through SH321. Interestingly, the increase of Type 3 crystals from SH304 (November 2004) to SH305 (January 3, 2005) correlates with an increase in magma

Table 3. Compositions of representative orthopyroxene phenocryst and acicular orthopyroxene inclusions in plagioclase phenocrysts.

[Features described as acicular inclusions are typical; those described simply as inclusions are also acicular but slightly larger. FeO*, total iron as Fe^{2+}. Molecular components for pyroxene shown calculated: En, enstatite; Fs, ferrosilite; Wo, wollastonite. Magnesium number, Mg# = (MgO×100)/(MgO+FeO*).]

	Phenocryst		Inclusion		Acicular Inclusion
	Core	Rim	Point 1	Point 2	Point 1
SiO_2	54.31	53.5	53.31	54.15	53.6
TiO_2	0.21	0.14	0.28	0.21	0.1
Al_2O_3	0.41	0.57	2.14	1.2	1.25
FeO*	21.38	23.74	20.02	20.66	23.17
MnO	0.66	0.79	0.47	0.44	0.76
MgO	23.72	21.68	23.45	23.57	22.08
CaO	0.86	0.73	1.59	1.24	0.73
En	65.3	61.0	65.5	65.4	62.0
Fs	33.0	37.5	31.4	32.2	36.5
Wo	1.7	1.5	3.2	2.5	1.5
Mg #	66.4	61.9	67.6	67.0	62.9

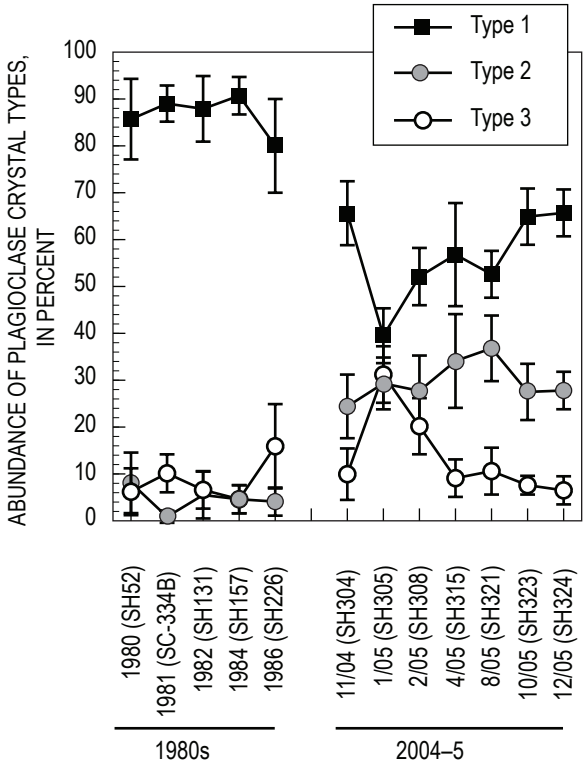

Figure 7. Proportions of different plagioclase types from crystal mapping. Bars showing 1σ error are based on variations measured among mapped sheets (25x images).

temperature as obtained from two-oxide geothermometry, whereas the tapering off to the initial abundance correlates with a drop in magma temperature in the spring of 2005 (Pallister and others, this volume, chap. 30). In other words, the sample in which crystals devoid of dissolution surfaces are most abundant is also the sample from which the highest temperature values were obtained. We will revisit this relation below.

Comparison of crystal populations of 2004–5 dacites with samples of 1980s dome dacite reveals a striking difference, even if all 2004–5 samples are averaged (fig. 7, table 1). The Type 2 crystals are sparse in 1980s dacite, which is dominated by Type 1 crystals. Type 3 crystals display comparable abundances except a temporary increase in samples collected in January and February 2005. In essence, the main difference between 2004–5 and 1980 dacites is an absence of orthopyroxene inclusions in 1980s lava.

Discussion

Acicular Orthopyroxene Inclusions as Probable Markers of Cooling Events

The presence of acicular orthopyroxene inclusions in plagioclase phenocrysts of the 2004–5 dacite is a striking feature (figs. 3, 4, 8). They are also present in plagioclase of 1980s dome dacite, although much rarer than in 2004–5 samples (table 1), and have since been observed by the first author elsewhere in andesite from Mount Hood, Oregon, and Volcán Arenal, Costa Rica. Thus, acicular orthopyroxene inclusions in plagioclase are not unique to this eruption, but their abundance and systematics of occurrence are presently unrivaled. Texturally identical orthopyroxene crystals occur in interstitial glass or groundmass in dacite of the current eruption, as well as in 1980s dome dacite (fig. 8). In particular, samples composed of interstitial glass laced by acicular orthopyroxene microlites and of scattered plagioclase microphenocrysts (<70 μm, either dimension) such as sample SH304-2G of the current eruption (Pallister and others, this volume, chap. 30) and SC99-334A (fig. 8), a 1981 sample, are important because they demonstrate that conditions exist in which interstitial melts of Mount St. Helens dacite primarily nucleate orthopyroxene that grew rapidly (as suggested by being acicular; for example, see Lofgren, 1980).

The supersaturation required to nucleate and rapidly grow orthopyroxene may be caused by a drop in temperature, by decompression associated with degassing, or by a combination of both. Samples with a more crystalline groundmass (for example, SH305-1, fig. 8) contain larger acicular orthopyroxene, which indicate that growth of acicular orthopyroxene continued as groundmass crystallinity increased. Plagioclase did not undergo a concurrent nucleation and rapid-growth event; instead of acicular crystals, equant plagioclase crystals continued to grow. Plagioclase growth in interstitial melt is strongly governed by the rate of decompression and devolatilization as magma ascends to the surface (Hammer and Rutherford,

2002). In general, rapid nucleation rate and acicular growth of plagioclase are induced by faster decompression and devolatilization rates. The occurrence of acicular groundmass orthopyroxene in the absence of acicular plagioclase in SH304-2G and SC99-334A (both representing magma seemingly saturated in orthopyroxene and plagioclase) suggests that temperature may have played an equal or more important role than decompression and devolatilization to induce supersaturation in orthopyroxene but not in plagioclase. Only slow and steady or small decompression steps are compatible with equant shapes of plagioclase microphenocrysts (Hammer and Rutherford, 2002).

An alternative interpretation, that a boundary layer enriched in orthopyroxene components rejected by growing plagioclase and subsequent local saturation and crystallization, is unlikely. A few orthopyroxene crystals may be generated this way but not the swarms of inclusions observed (fig. 8). Constant or decreasing Fe content in profiles approaching bands of orthopyroxene inclusions (fig. 8*D*) suggests no major enrichment of total Fe in the boundary layer.

In conclusion, we believe that the presence of acicular orthopyroxene in some plagioclase phenocryst bands reflects an abundance of acicular orthopyroxene microlites in the interstitial melt at the time of embedding. Therefore, acicular orthopyroxene-rich zones in plagioclase record rapid orthopyroxene-nucleation events that were probably induced in large part by rapid cooling.

Production of Near-Rim Plagioclase—an Evaluation of Processes and Natural Constraints

Cooling, decompression, compositional and volatile fluxes, and kinetic effects all may control compositional and textural features of plagioclase—although we consider kinetic effects (for example, see Pearce, 1994) at best a secondary cause for the abrupt increase of An content by more than 2–4 mol percent (for example, see Ginibre and others, 2002). It is

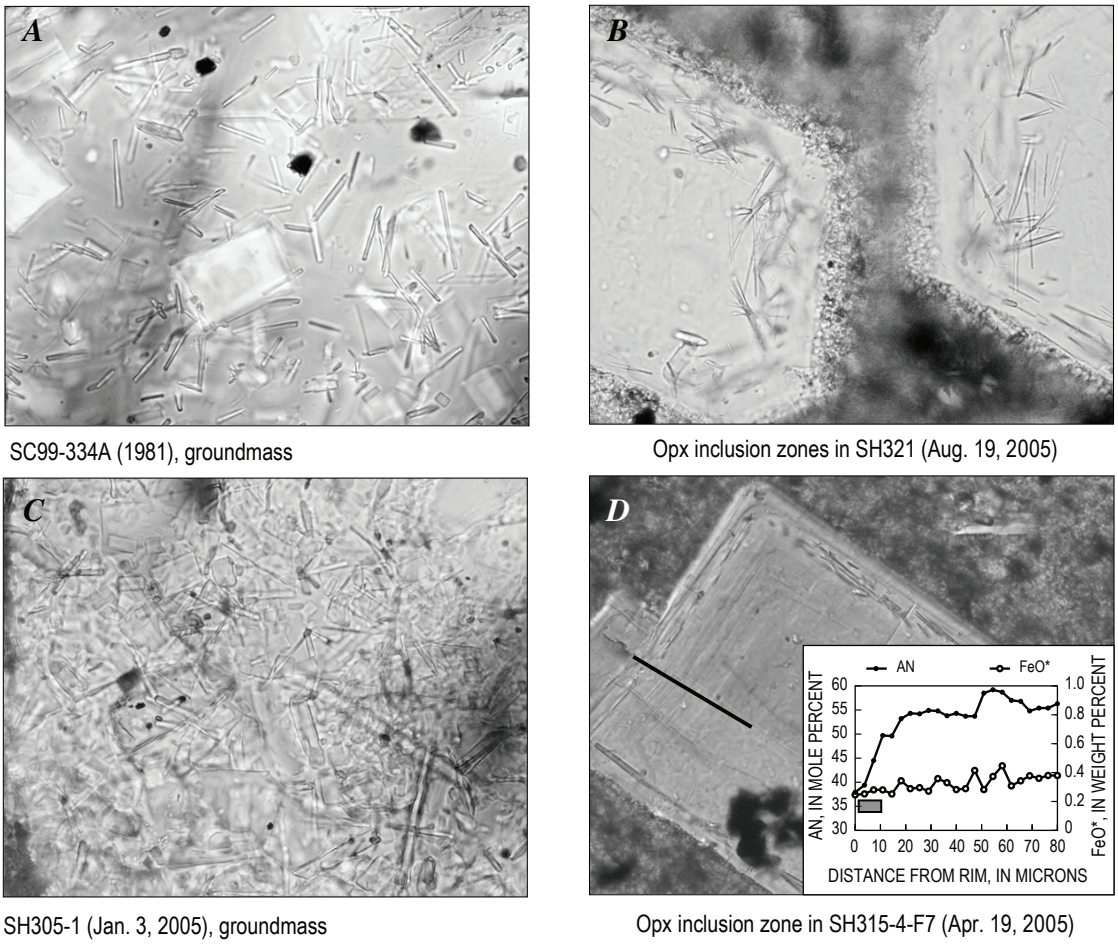

SC99-334A (1981), groundmass

Opx inclusion zones in SH321 (Aug. 19, 2005)

SH305-1 (Jan. 3, 2005), groundmass

Opx inclusion zone in SH315-4-F7 (Apr. 19, 2005)

Figure 8. Occurrence of acicular orthopyroxene crystals in groundmass (*A*, *C*) and as inclusions in plagioclase (*B*, *D*). All pictures in transmitted light. *A* and *C* at x 1000 magnification, *B* at x 500 magnification, and *D* at x 200 magnification. Inset in *D* shows analysis traverse along solid line.

typically a certain combination of features that narrows down which parameter exerted greater control.

Below we make the case that the characteristic features of Types 1 and 2 crystals—multiple, normally zoned bands separated by dissolution surfaces within the outer ~80 μm of crystals, combined with marked declines in An content within variably thick bands (as thin as 10–20 μm)—are most consistent with fluctuations in crystallinity as primarily induced by temperature, with other parameters contributing in secondary roles. On the other hand, normal zoning (that is, progressive outward decrease of An content toward rim) over wider (>~50 μm) distances without dissolution surfaces—as observed in Type 3 crystals—is less constrained and may record times when other parameters such as pressure outweigh temperature changes.

If the magmatic system were closed, then higher and lower An content would imply lower or higher crystallinity, respectively, at the time of crystallization. To correlate the degree of crystallinity with a particular An content in plagioclase, we calculated melt composition at a variety of crystallinities and varied the partition coefficient, Kd (Kd = Ca/Na_{plag}/Ca/Na_{melt}) (Sisson and Grove, 1993), to calculate equilibrium compositions of plagioclase (fig. 9). For our model calculations, we used an average bulk composition from initial anlyses of November 4, 2004, dacite (SH304) as starting composition (final analyses in Thornber and others, 2008b). A fixed mineral assemblage was removed from the bulk composition to calculate interstitial melt composition. The assemblage consisted of 6 percent amphibole, 9 percent orthopyroxene, 18 percent An_{53} plagioclase, 65 percent An_{42} plagioclase, and 2 percent titanomagnetite and is based on mineral modes established for 2004–5 dacite (Pallister and others, this volume, chap. 30). Although the extraction oversimplifies any natural process, certain important features are illustrated. If SH304 ever existed as pure liquid, it would initially crystallize An_{53} (at Kd=2) to An_{75} (at Kd=5) under lower to higher water-saturated conditions, respectively (Sisson and Grove, 1993) (fig. 9). We estimate that our investigation applies to approximately the last 30–40 percent of plagioclase phenocryst crystallization (synonymous with whole-rock crystallinities above ~30 percent), as suggested by lengths of microprobe traverses combined with range of phenocryst sizes studied. Thus, the highest commonly observed An content of 55 to 60 mol percent was achieved when crystallinity of SH304 dacite was already at or near 30 percent. This crystallinity requires a minimum Kd of 3, or higher at higher crystallinities, in order to generate $An_{55–60}$ at water-saturated conditions (fig. 9), an interpretation supported by water-saturated experimental results obtained on dacite SH305, in which conditions of 870ºC and 200 MPa produced An_{50} plagioclase at a crystallinity of ~30 percent (Rutherford and Devine, this volume, chap. 31). On the other hand, an An content of 37 mol percent requires crystallinity near 50 percent, in keeping with the observation that 2004–5 dacite consists of ~45 percent groundmass (interstitial glass and/or groundmass crystals), and An_{37} is the typical rim and microphenocryst composition. As a consequence, crystals that have equally low or even lower An content further inward than at the rim (figs. 4, 5, 6) mark earlier times when crystal growth occurred at crystallinities between 50 and 60 percent.

A decrease of An content from 55 to 37 mol percent, as is observed commonly within single compositionally zoned bands, requires the following conditions or some combination thereof: (1) ~25 percent crystallization at constant Kd or (2) decreasing Kd at constant crystallinity (for example, at 40 percent crystallinity, Kd would need to decrease from ~4.5 to 2). A decrease in Kd at water-saturated conditions and a given melt composition is synonymous with a decrease in water concentration and thus decrease in P_{total} (Sisson and Grove, 1993). To explain crystals with several dissolution surfaces by changes in Kd would be problematic, as changes in Kd would need to be dramatic and cyclic. If Kd exerted a dominant control on observed An content, then a return to $An_{50–55}$ after resorption would require a substantially higher Kd and would require the crystal to return to a greater depth (Hattori and Sato, 1996). Water-saturated experiments indicate that an increase in pressure of 60 MPa would increase An content by 5 mol percent in Mount St. Helens dacite magmas (Rutherford and Devine, this volume, chap. 31). Thus crystals with bands with An contents ≥5 mol percent higher after resorption would require a depth increase of ~2 km or more, and crystals that display several such bands would have been cycled numerous times. In fact, to

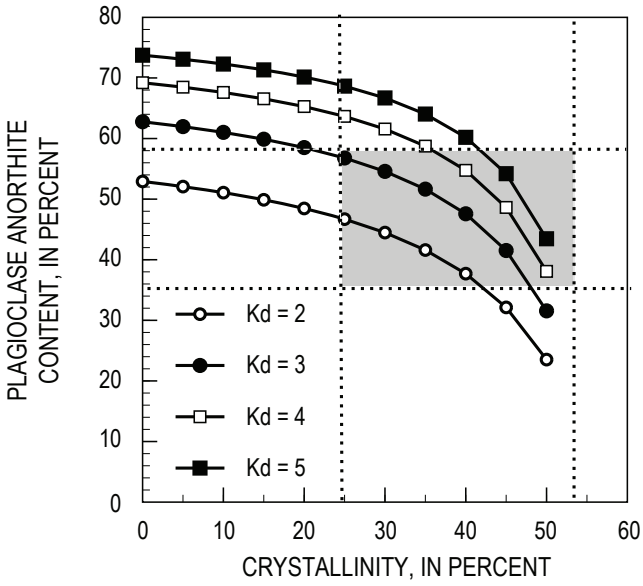

Figure 9. Variation of An content in plagioclase versus degree of crystallinity based on model calculations using variable Kd (=(Ca/Na_{plag})/(Ca/Na_{melt})), bulk composition of SH304 as starting composition (table 1), and removal of a fixed mineral assemblage (see text for details). Model simulates correlation of degree of crystallinity with plagioclase An composition in equilibrium with corresponding interstitial melt. Shaded zone marks conditions covered by this study, as suggested by lengths of microprobe traverses combined with range of phenocryst sizes investigated.

explain the entire An range of An_{55} to An_{37} would require pressure to fluctuate by 150 MPa, equivalent to a depth change of ~5.5 km (Rutherford and Devine, this volume, chap. 31).

An additional complicating factor is that once magma has reached water saturation and begins to degas at shallow depth, it will become undersaturated as it reaches greater depths unless volatiles are added to keep it saturated. If it did not gain volatiles, descent towards higher degree of undersaturation would promote crystallization as the liquidus is raised and likely would crystallize plagioclase of lower An content (for example, Blundy and Cashman, 2001). To return multiple times from An_{37} to An_{55} at a constant Kd poses comparably little difficulty. The only requirement is that crystallinity needs to fluctuate by ~25 percent or less to return to an An content of An_{55}; this could be achieved by local cooling and subsequent entrainment into more interior and hotter parts of the magmatic reservoir (Singer and others, 1995; Couch and others, 2001). In fact, Rb concentrations in melt inclusions of 1980s dacite suggest crystallinity variation by 20 percent at a constant pressure over the pressure interval from 200 to 100 MPa (Blundy and others, 2006)—the inferred pressure of the upper part of the 2004–5 magmatic reservoir (Pallister and others, this volume, chap. 30). A temperature change of about 45ºC would be needed to achieve this, consistent with experimental results showing that An_{55} plagioclase crystallizes at 890ºC and An_{37} crystallizes at 845ºC (Rutherford and Devine, this volume, chap. 31). Such temperatures are also within the range deduced from oxide geothermometry of 2004–5 dacite (Pallister and others, this volume, chap. 30) and are similar to isobaric variations deduced from plagioclase-liquid geothermometry on 1980s dacite (Blundy and others, 2006). Latent heat of crystallization (Blundy and others, 2006) may have contributed to the increase in temperature. On the other hand, magma heating by decompression-driven crystallization (Blundy and others, 2006) appears minimal above 50 MPa and is most significant from about 40 MPa to the surface. Therefore the greatest impact of latent heat is taking place at pressure significantly shallower than conditions of the magma reservoir. Consequently, variation of magma temperatures observed at pressures above 50 MPa require additional explanation (see section "New Versus 1980s Residual Magma and Evidence for Magmatic Recharge," below).

Returning to the discussion of our compositional data, alternative possibilities under conditions of an open system (that is, involving magma and (or) volatile flux into or out of the system) include: (1) an influx of higher Ca/Na magma and (2) switching between water-undersaturated and saturated conditions as the system ranges between lithostatic and hydrostatic conditions. The latter is the only instance where a decrease in P_{total} is not synonymous with decreasing depth as the system degasses under hydrostatic conditions and then is repressurized as connection to the surface ceases and the system returns to lithostatic conditions. Periodic influx (recharge) of more mafic (higher Ca/Na) magma may help to reset conditions for crystallization of a more An-rich plagioclase onto dissolution surfaces, and there is circumstantial evidence that this effect is occurring (see section "New Versus 1980s Residual Magma and Evidence for Magmatic Recharge"). Furthermore, this mechanism works in concert with the notion that abrupt near-rim decrease in An content within single bands is driven mostly by increased crystallinity owing to cooling. The other possibility—in essence reflecting shallow and periodic degassing events—has been advocated to occur at El Chichón volcano during eruption and repose cycles (Tepley and others, 2000). Degassing would promote crystallization, and resorption would then need to occur during repressurization of the system. This process may have contributed to features observed in plagioclase of the 2004–5 dacite at Mount St. Helens (see below) but cannot serve as sole explanation as clearly evidenced by juxtaposed plagioclase phenocrysts with no, single, or multiple dissolution surfaces, therefore requiring a range in the number of degassing events.

Crystal Histories and Populations

On the basis of our textural and compositional analysis, it appears that all plagioclase phenocrysts share, at best, only the last An decrease over the last 5–20 μm. Thus, it seems impossible to generate the diverse features in plagioclase described above during a single ascent in which essentially all phenocrysts grow—as is envisioned for plagioclase of the dome dacite of the 1980s (Blundy and Cashman, 2001). It appears that the only plagioclase crystals for which a single-ascent history is conceivable are crystals that display monotonically decreasing An content (our Type 3) and probably crystals that show mostly continuously decreasing An content but with a dissolution surface deeper in the core of the crystal. These could be a product of continuous crystallization driven by decompression (Blundy and Cashman, 2001). In our view, plagioclase crystals that are poorly explained by a continuous ascent-driven crystallization are those with multiple, normally zoned bands separated by dissolution surfaces. Nearly isobaric temperature fluctuations (corresponding to degree of crystallinity) could account for multiple dissolution surfaces as discussed above. On the other hand, such zonation patterns (also known as sawtooth patterns) have recently been attributed to processes of magma heating by decompression-driven crystallization (Blundy and others, 2006). As argued above, such processes are strongest at depths of less than 1 km and therefore would occur in the conduit and would impact all plagioclase during their final ascent.

In the discussion of crystal populations, two important questions concern the significance of any recognized crystal population and the significance of variations from it. The answers to both questions depend on the processes controlling the features that define crystal types, the minimal changes needed to induce these features, and the minimal distances needed to see a response to differing environmental conditions. As presented above, we based our crystal types on existence of dissolution surfaces separating growth bands and the presence of acicular orthopyroxene. This is analogous to plagioclase

crystal populations established by Pearce and others (1987) for dacite of May 18, 1980. The abundance of dissolution surfaces in plagioclase from Mount St. Helens dacite and from dacite elsewhere (for example, see Pearce, 1994) suggests that these features do not require major changes in magmatic conditions but are produced rather easily. Therefore, neighboring crystals with a variable number of dissolution surfaces likely experienced different growth histories and were subsequently juxtaposed by mixing. We propose that crystals with no dissolution surface are those that were supplied to the erupting dacite magma last, whereas increasingly more complex textures, especially several zoned bands bound by dissolution surfaces, are evidence of a prolonged residency and evolution in a shallow reservoir (for example, Tepley and others, 2000). Crystals with multiple bands can be explained solely by temperature gradients and, thus, by crystallinity gradients across the reservoir, in combination with recharge by higher Ca/Na melt (fig. 10). Cycling through polybaric conditions, seemingly required to explain amphibole compositions in 2004–5 dacite (Rutherford and Devine, this volume, chap. 31), is permissible as an influence on the development of bands and zonation. However, narrow (~10–15 μm) bands with strong zonation (for example, ΔAn ≥10 mol percent), which suggest rapid, back-and-forth changes in growth conditions, argue against pressure as a principal control because the required cycling through a vertical distance of several kilometers (~4 km) is unrealistic.

New Versus 1980s Residual Magma and Evidence for Magmatic Recharge

One of the main questions asked about the renewed activity at Mount St. Helens is whether dacite lava that has extruded since October 2004 is magma that was stored in the subvolcanic reservoir since Mount St. Helens erupted in 1986 or is freshly supplied magma. Bulk chemical analyses demonstrate that there are chemical differences between 1980s and 2004–5 lava; for example, SiO_2 is about 1.5–2.5 wt. percent higher in 2004–5 dacite than in most 1980s dome dacite (Pallister and others, this volume, chap. 30). Results from our crystal mapping hold clues to answering the question of new versus residual magma. The high ratio of Type 1 to Type 2 crystals in 1986 versus 2004–5 lava in general and the higher proportion of Type 3 crystals in January and February 2005 samples (table 1, fig. 7) suggest that lava extruded during the current activity is not from the same magma that was extruded during the final year of dome growth in 1986. Closed-system evolution from 1986 to today is one conceivable possibility to explain the observed differences in plagioclase phenocryst populations. Yet, any increases in Type 3 crystals in 2004–5 lava cannot be due to modification of crystals with dissolutions surfaces, which makes the higher proportion of Type 3 crystals early in the 2004–5 eruption in comparison to 1980s sample indicative of freshly supplied crystals. Furthermore, to explain increases in the ratio of Type 2 to Type 1 crystals by growth evolution since 1986, the following would be required: crystallization to trap orthopyroxene followed by some resorption, in turn followed by crystallization of more plagioclase. From the above, it seems likely that 2004–5 dacite is composed mostly of variable proportions of magmatic components that have undergone shallow evolution (that is, modified, residual magma) and components that have been added from deeper parts (new magma). In other words, various magmatic sources provided plagioclase phenocrysts to explain multiple crystal histories, and phenocrysts were juxtaposed by mixing events (additionally, crustal sources supplied xenocrystic plagioclase, but we neglect these in the discussion here).

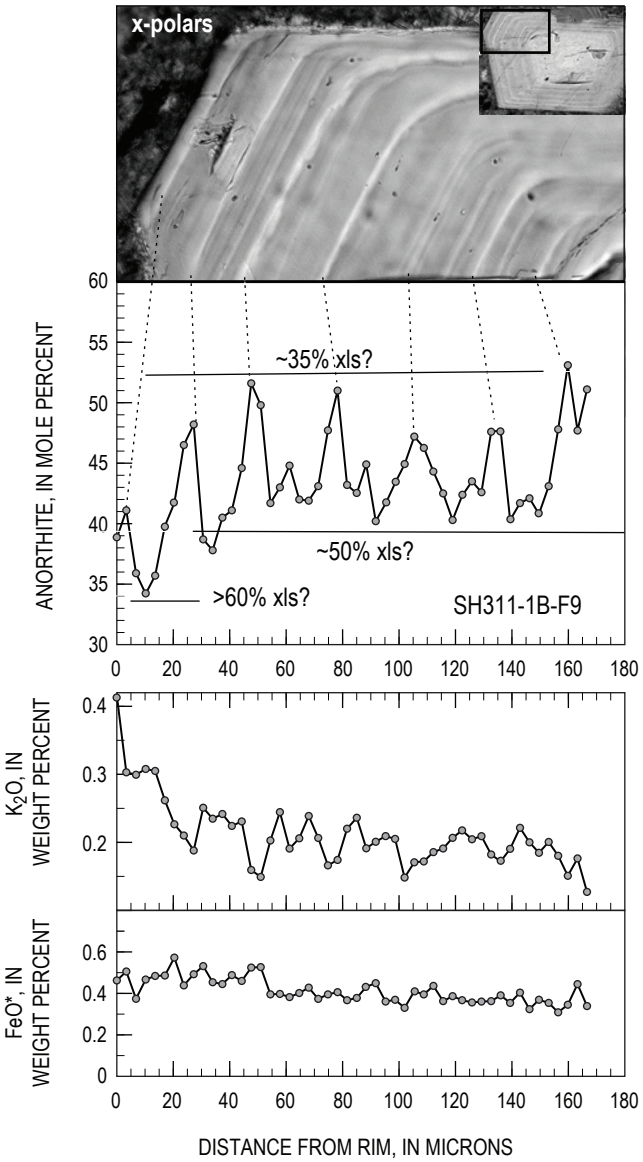

Figure 10. Analytical traverse of plagioclase SH311-1B-F9 showing multiple normally zoned bands bounded by mild dissolution (resorption) surfaces. An peaks correlate inversely with K but not with Fe. We propose that highest An contents record magmatic conditions of low crystallinities (~35 percent crystals) whereas low An contents record high crystallinities (50–60 percent crystals). FeO*, total iron as Fe^{2+}.

There is additional circumstantial evidence that the current eruption has experienced magmatic recharge by hotter magmas with more calcic melts (but not necessarily more calcic bulk composition). Assume that a magma batch undergoes closed-system crystallization to produce the same growth features in equally sized crystals. If growth were continuous, we would expect decreasing An content in the plagioclase crystals as fractional crystallization progresses and the melt fraction decreases (if crystal-melt equilibrium is not maintained). If the same system were to oscillate between higher and lower crystallinity during its course of crystallization, owing to temperature fluctuations, we would expect profiles of overall An decrease toward crystal rims but modulated by resorption and precipitation of higher-An bands (Pearce, 1994; Johannes and others, 1994). Partial plagioclase dissolution would raise the Ca/Na in the melt, and therefore initial overgrowth would be higher in An content than that before resorption. The An content of the initial overgrowth will depend on how much dissolution occurred and may be also influenced by nonequilibrium crystallization effects related to the kinetics of the system (Stewart and Fowler, 2001), but it could never return to the most calcic composition unless all plagioclase dissolved (neglecting the effect of volumetrically less significant calcic phases, for example hornblende or augite, on Ca/Na ratios). Subsequent growth would rapidly decrease An content to lower values as the system increased in crystallinity. This plagioclase response is illustrated schematically in figure 11 as profile A, which is rarely seen in plagioclase of the current

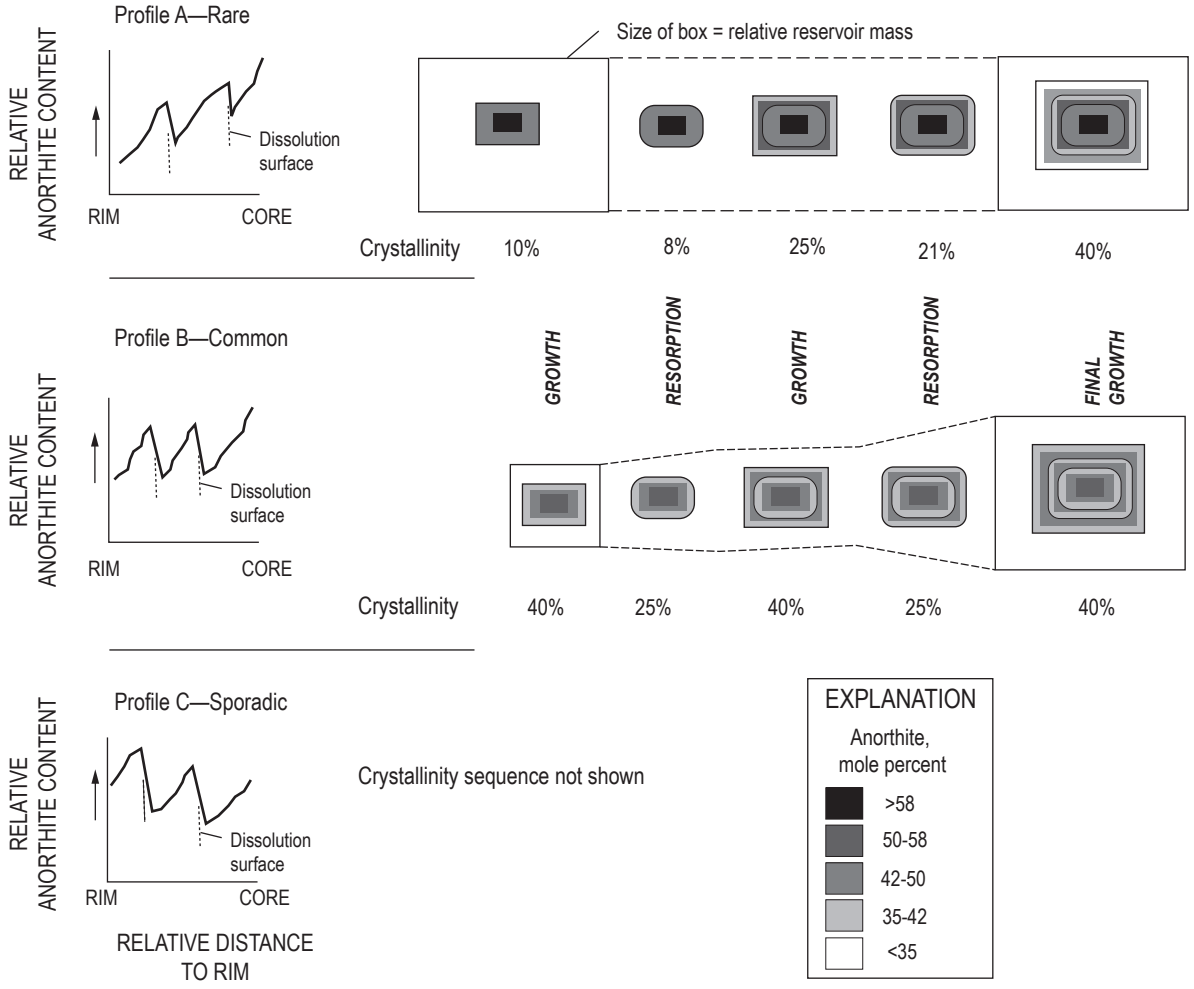

Figure 11. Schematic scenarios to produce common An profiles observed in 2004–5 plagioclase. Given An ranges shown in legend and crystallinity proportions are approximate values. To generate profile B, often observed in plagioclase of 2004–5 dacites, probably requires influx of melt (that is, an increase in reservoir mass) to buffer Ca/Na. If a closed system were to fluctuate in its degree of crystallinity due to temperature variations, profile A would be expected to result, which is only rarely observed. We therefore propose that profile B and, even more so, profile C, are likely the signs of a recharged system rather than one that is closed for magma input.

eruption but is common elsewhere (for example, Tatara dacite, see Singer and others, 1995). A common An profile among 2004–5 phenocrysts, profile B (fig. 11), shows An oscillations with minima and maxima immediately inward and outward of the dissolution surface, respectively, and the range of An content is similar over the course of crystallization (fig. 10). This constant An range is important because, as plagioclase on the whole crystallizes, the system can only produce similar An maxima if there is an influx of melt to buffer melt Ca/Na. The influx needed depends on the Ca/Na ratio in the melt that is recharged and other phases that may be crystallizing. In general, this requires an open system in which the overall crystal mass increases but where melts are buffered to produce the same An range during crystallization of multiple bands (fig. 10). Plagioclase simply convecting through a thermal regime (Singer and others, 1995) would not work because, if balanced, the amount of crystallization on a cooling path and the amount of resorption during the heating stage would not yield an overall growing crystal with return to similar An minima and maxima unless some phenocrysts grow while others are increasingly dissolved, for which evidence is lacking. Shifting crystallization to progressively lower pressures over the course of growth of multiple bands would make it increasingly more difficult to return to comparable An maxima. Plagioclase crystals with compositional profiles similar to schematic profile C (fig. 11)—with a baseline composition that is more calcic towards rim—carry even stronger evidence for an open-system behavior concurrently and (or) preceding the 2004–5 extrusion of dacite magma. The only alternate explanation for crystals to oscillate compositionally around comparable An minima and maxima or around an increasing An baseline with time during ~30 percent of plagioclase crystallization (fig. 10) appears to be decompression-driven crystallization in a heating environment (Blundy and others, 2006). However, the lack of a rim overgrowth of high An on all crystals during the last ascent of 1,000 m (that is, where this affect would be strongest; fig. 2a in Blundy and others, 2006) and the observed low An of tiny microphenocrysts of this study (for example, figs. 6, 8*A*) rather excludes the "latent-heat" explanation. We therefore take the compositional features of profiles B and C (fig. 11) as evidence for magma recharge either of hotter and less crystalline dacitic magma of similar bulk composition as the 2004–5 eruption or of more mafic, Ca-richer magma that has not yet been sampled as extruded lava. Dissolution of plagioclase from gabbroic xenoliths may help buffer Ca/Na as well, but only if the system is sufficiently hot.

Plagioclase View of the Mount St. Helens Eruption

On the basis of the discussion above, we infer the following. Subsequent to the last extrusive event in 1986, remaining dacite magma began cooling. Crystal growth was intermittent as crystals cycled through the interior, hotter parts of the reservoir/conduit system, causing resorption. Temperature gradients across the reservoir were possibly maintained by minor recharge events of deeper dacite magma, which also supplied some plagioclase phenocrysts that were subjected to the same subsequent cycles of resorption and growth as the resident crystals. Seismic evidence also suggests that recharge may have occurred in the middle to late 1990s (Moran and others, this volume, chap. 2). Prior to the renewed eruptive activity in 2004, a relatively widespread crystallization event caused growth and incorporation of acicular orthopyroxene inclusions as some magma experienced rapid cooling, possibly associated with ascent. Subsequent arrival and mixing of new dacite magma remobilized more crystalline parts of the system, causing resorption as new magma mixed with resident magma, ultimately causing the final ascent to the surface immediately or within weeks. During the final ascent, crystals grew euhedral rims. We attribute the last growth cycle—in which plagioclase of lowest An content incorporates acicular orthopyroxene inclusions, is partially resorbed, overgrown with higher An content, and subsequently normally zoned—to magmatic processes that triggered the onset of extrusion in October 2004; but it predated the eruption by months to weeks. Some (as many as three?) of the older, more interior dissolution surfaces, but still within the outer ~80 μm of crystals, may postdate the last eruption in 1986 but predate the last growth cycle. Simply zoned crystals with continuously decreasing An content (that is, Type 3 crystals) were carried by recharging dacite, grew largely in response to decompression, and thus may track the amount of recharged magma. They were stirred into the residing magma and, together with already existing phenocrysts, underwent crystallization to develop a common growth history during final ascent. Earlier recharge events may have carried similar plagioclase but, unless erupted immediately, that plagioclase was texturally modified by resorption-and-growth events, thereby losing its distinct textural character. This model is compatible with results from other petrologic studies of 2004–5 dacite (this volume: Pallister and others, chap. 30; Rutherford and Devine, chap. 31; Thornber and others, chap. 32; Cooper and Donnelly, chap. 36; Reagan and others, chap. 37).

Conclusions

We investigated plagioclase, focusing on near-rim areas of phenocrysts in dacite of the 2004–5 eruption, and compared those to plagioclase in selected dacite samples from the dome that grew in the 1980s. The results of our textural and compositional study are the following:

1. On the basis of distinguishing several plagioclase textural types in combination with a newly developed crystal mapping procedure, we show that 2004–5 dacite contains a different crystal population than 1980s dacite.

2. Observed An range of plagioclase near rim (≤80 μm) in 2004–5 dacite is $An_{57–35}$, and minima correspond with compositions of smallest microphenocrysts (≤20 μm) at overall crystal contents of ~50 percent. Location of

a given An composition is largely independent of the distance to the rim of crystals, except in texturally simple crystals without dissolution surfaces that are normally zoned (that is, highest An content in innermost reach and lowest An content at the rim). Crystals with dissolution surfaces possess normal zonation within bands bounded by dissolution surfaces, so that highest An content is the immediate overgrowth on a dissolution surface and lowest An content within a band is last to crystallize, leading to one or several An oscillations toward the rim.

3. Acicular orthopyroxene inclusions in plagioclase are characteristic of 2004–5 dacite, and they are consistently embedded in plagioclase with lowest An content. Orthopyroxene inclusions have textural counterparts in glassy groundmass of a rare 2004 sample and also in samples from the 1980s. The orthopyroxene occurrences suggest that inclusions in plagioclase track previous magmatic conditions at which acicular orthopyroxene crystals were temporarily abundant in interstitial melt.

4. We attribute An oscillations with comparable An minima and maxima mostly to changes in crystallinity as induced largely by temperature fluctuations in combination with recharge to maintain Ca/Na as crystallization generally progresses. Plagioclase of lowest An content and with acicular orthopyroxene inclusions may record higher crystallinity and lower temperature conditions (lower Ca/Na in melt), whereas plagioclase of highest An content overgrowing dissolution surfaces crystals may track conditions of lower crystallinity and higher temperature (higher Ca/Na in melt). Convection along a pressure gradient may aid the process through ascent-induced crystallization and descent-induced resorption. Crystals with normal An zonation and essentially no dissolution surface likely crystallized entirely in a decompressing environment.

5. The assemblage of phenocrysts with one or more growth bands composed of similar An range requires localized and repetitive processes, including mixing, to juxtapose crystals with different growth histories. Crystallization of the outermost ~5–15 μm developed during a common growth history among phenocrysts.

6. We envision a scenario in which residual 1980s magma continued to evolve subsequent to the last extrusion in 1986 and was maintained by small recharge events. A cycle of pronounced cooling/heating/cooling (possibly associated with ascent) shortly (months?) before the current eruptive activity can be inferred from the characteristic textural features of 2004–5 plagioclase, namely acicular orthopyroxene inclusions embedded prior to the last dissolution surface, which in turn was overgrown by euhedral rims. Our data are compatible with recharge-driven initiation of the current eruption and that recharged magma may also be dacitic but poorer in crystals and hotter than resident dacite into which it has been blended.

Acknowledgments

We acknowledge support for the remote-access electron microprobe laboratory at Portland State University through a National Science Foundation grant, EAR-0320863. M.J. Streck acknowledges support from the Eidgenössische Technische Hochschule (ETH) Zürich as Gastdozent (guest professor) during preparation of this manuscript and thanks W. Halter and C. Heinrich at the ETH and H.-J. Massone and T. Theye at the University of Stuttgart for their hospitality. Reviews by Maggie Mangan and Frank Tepley were very helpful and improved the paper significantly.

References Cited

Blundy, J., and Cashman, K., 2001, Ascent-driven crystallisation of dacite magmas at Mount St. Helens, 1980–1986: Contributions to Mineralogy and Petrology, v. 140, no. 6, p. 631–650, doi:10.1007/s004100000219.

Blundy, J., Cashman, K., and Humphreys, M., 2006, Magma heating by decompression-driven crystallization beneath andesite volcanoes: Nature, v. 443, no. 7107, p. 76–80, doi:10.1038/nature05100.

Cashman, K.V., 1992, Groundmass crystallization of Mount St. Helens dacite, 1980–1986; a tool for interpreting shallow magmatic processes: Contributions to Mineralogy and Petrology, v. 109, no. 4, p. 431–449, doi:10.1007/BF00306547.

Clynne, M.A., Calvert, A.T., Wolfe, E.W., Evarts, R.C., Fleck, R.J., and Lanphere, M.A., 2008, The Pleistocene eruptive history of Mount St. Helens, Washington, from 300,000 to 12,800 years before present, chap. 28 *of* Sherrod, D.R., Scott, W.E., and Stauffer, P.H., eds., A volcano rekindled; the renewed eruption of Mount St. Helens, 2004–2006: U.S. Geological Survey Professional Paper 1750 (this volume).

Cooper, K.M., and Donnelly, C.T., 2008, ^{238}U-^{230}Th-^{226}Ra disequilibria in dacite and plagioclase from the 2004–2005 eruption of Mount St. Helens, chap. 36 *of* Sherrod, D.R., Scott, W.E., and Stauffer, P.H., eds., A volcano rekindled; the renewed eruption of Mount St. Helens, 2004–2006: U.S. Geological Survey Professional Paper 1750 (this volume).

Couch, S., Sparks, R.S.J., and Carroll, M.R., 2001, Mineral disequilibrium in lavas explained by convective self-mixing in open magma chambers: Nature, v. 411, p. 1037–1039.

Gerlach, T.M., McGee, K.A., and Doukas, M.P., 2008, Emission rates of CO_2, SO_2, and H_2S, scrubbing, and preeruption excess volatiles at Mount St. Helens, 2004–2005, chap. 26 *of* Sherrod, D.R., Scott, W.E., and Stauffer, P.H., eds., A volcano rekindled; the renewed eruption of Mount St. Helens, 2004–2006: U.S. Geological Survey Professional Paper 1750 (this volume).

Ginibre, C., Kronz, A., and Wörner, G., 2002, High resolution quantitative imaging of plagioclase composition using accumulated backscattered electron images; new constraints on oscillatory zoning: Contributions to Mineralogy and Petrology, v. 142, p. 436–448.

Hammer, J.E., and Rutherford, M.J., 2002, An experimental study of the kinetics of decompression-induced crystallization in silicic melt: Journal of Geophysical Research, v. 107, no. B1, p. ECV 8-1–8-24, doi:10.1029/2001JB000281.

Hattori, K., and Sato, H., 1996, Magma evolution recorded in plagioclase zoning in 1991 Pinatubo eruption products: American Mineralogist, v. 81, p. 982–994.

Heliker, C., 1995, Inclusions in the Mount St. Helens dacite erupted from 1980 through 1983: Journal of Volcanology and Geothermal Research, v. 66, nos. 1–3, p. 115–135, doi:10.1016/0377-0273(94)00074-Q.

Herriott, T.M., Sherrod, D.R., Pallister, J.S., and Vallance, J.W., 2008, Photogeologic maps of the 2004–2005 Mount St. Helens eruption, chap. 10 *of* Sherrod, D.R., Scott, W.E., and Stauffer, P.H., eds., A volcano rekindled; the renewed eruption of Mount St. Helens, 2004–2006: U.S. Geological Survey Professional Paper 1750 (this volume).

Johannes, W., Koepke, J., and Behrens, H., 1994, Partial melting reactions of plagioclase and plagioclase-bearing systems, *in* Parsons, I., ed., Feldspars and their reactions: Dordrecht, Netherlands, Kluwer Academic Publishers, NATO Advanced Study Institute series, v. 421, p. 161–194.

Lofgren, G., 1980, Experimental studies on the dynamic crystallization of silicate melts, *in* Hargraves, R.B., ed., Physics of magmatic processes: Princeton, New Jersey, Princeton University Press, p. 478–551.

Moran, S.C., Malone, S.D., Qamar, A.I., Thelen, W.A., Wright, A.K., and Caplan-Auerbach, J., 2008, Seismicity associated with renewed dome building at Mount St. Helens, 2004–2005, chap. 2 *of* Sherrod, D.R., Scott, W.E., and Stauffer, P.H., eds., A volcano rekindled; the renewed eruption of Mount St. Helens, 2004–2006: U.S. Geological Survey Professional Paper 1750 (this volume).

Pallister, J.S., Thornber, C.R., Cashman, K.V., Clynne, M.A., Lowers, H.A., Mandeville, C.W., Brownfield, I.K., and Meeker, G.P., 2008, Petrology of the 2004–2006 Mount St. Helens lava dome—implications for magmatic plumbing and eruption triggering, chap. 30 *of* Sherrod, D.R., Scott, W.E., and Stauffer, P.H., eds., A volcano rekindled; the renewed eruption of Mount St. Helens, 2004–2006: U.S. Geological Survey Professional Paper 1750 (this volume).

Pearce, T.H., 1994, Recent work on oscillatory zoning in plagioclase, *in* Parsons, I., ed., Feldspars and their reactions: Dordrecht, Netherlands, Kluwer Academic Publishers, NATO Advanced Study Institute series, v. 421, p. 313–349.

Pearce, T.H., Russell, J.K., and Wolfson, I., 1987, Laser-interference and Nomarski interference imaging of zoning profiles in plagioclase phenocrysts from the May 18, 1980, eruption of Mount St. Helens, Washington: American Mineralogist, v. 72, p. 1131–1143.

Reagan, M.K., Cooper, K.M., Pallister, J.S., Thornber, C.R., and Wortel, M., 2008, Timing of degassing and plagioclase growth in lavas erupted from Mount St. Helens, 2004–2005, from ^{210}Po-^{210}Pb-^{226}Ra disequilibria, chap. 37 *of* Sherrod, D.R., Scott, W.E., and Stauffer, P.H., eds., A volcano rekindled; the renewed eruption of Mount St. Helens, 2004–2006: U.S. Geological Survey Professional Paper 1750 (this volume).

Rutherford, M.J., and Devine, J.D., III, 2008, Magmatic conditions and processes in the storage zone of the 2004–2006 Mount St. Helens dacite, chap. 31 *of* Sherrod, D.R., Scott, W.E., and Stauffer, P.H., eds., A volcano rekindled; the renewed eruption of Mount St. Helens, 2004–2006: U.S. Geological Survey Professional Paper 1750 (this volume).

Singer, B.S., Dungan, M.A., and Layne, G.D., 1995, Textures and Sr, Ba, Mg, Fe, K, and Ti compositional profiles in volcanic plagioclase; clues to the dynamics of calc-alkaline magma chambers: American Mineralogist, v. 80, p. 776–798.

Sisson, T.W., and Grove, T.L., 1993, Experimental investigations of the role of H_2O in calc-alkaline differentiation and subduction zone magmatism: Contributions to Mineralogy and Petrology, v. 113, p. 143–166.

Stewart, M.L., and Fowler, A.D., 2001, The nature and occurrence of discrete zoning in plagioclase from recently erupted andesitic volcanic rocks, Montserrat: Journal of Volcanology and Geothermal Research, v. 106, p. 243–253.

Tepley, F.J., III, Davidson, J.P., Tilling, R.I., and Arth, J.G., 2000, Magma mixing, recharge and eruption histories recorded in plagioclase phenocrysts from El Chichón volcano, Mexico: Journal of Petrology, v. 41, no. 9, p. 1397–1411, doi:10.1093/petrology/41.9.1397.

Thornber, C.R., Pallister, J.S., Lowers, H.A., Rowe, M.C., Mandeville, C.W., and Meeker, G.P., 2008a, Chemistry, mineralogy, and petrology of amphibole in Mount St. Helens 2004–2006 dacite, chap. 32 *of* Sherrod, D.R., Scott, W.E., and Stauffer, P.H., eds., A volcano rekindled; the renewed eruption of Mount St. Helens, 2004–2006: U.S. Geological Survey Professional Paper 1750 (this volume).

Thornber, C.R., Pallister, J.S., Rowe, M.C., McConnell, S., Herriott, T.M., Eckberg, A., Stokes, W.C., Johnson Cornelius, D., Conrey, R.M., Hannah, T., Taggart, J.E., Jr., Adams, M., Lamothe, P.J., Budahn, J.R., and Knaack, C.M., 2008b, Catalog of Mount St. Helens 2004–2007 dome samples with major- and trace-element chemistry: U.S. Geological Survey Open-File Report 2008–1130, 9 p., with digital database.